Modelling of NO destruction in a low-pressure reactor by an Ar plasma jet: species abundances in the reactor

2011 J. Phys. D: Appl. Phys. 44 105202

(http://iopscience.iop.org/0022-3727/44/10/105202)

IOP PUBLISHING JOURNAL OF PHYSICS D: APPLIED PHYSICS

J. Phys. D: Appl. Phys. **44** (2011) 105202 (9pp) doi:10.1088/0022-3727/44/10/105202

Modelling of NO destruction in a low-pressure reactor by an Ar plasma jet: species abundances in the reactor

Kinga Kutasi

Research Institute for Solid State Physics and Optics, Hungarian Academy of Sciences, POB 49, H-1525 Budapest, Hungary

E-mail: kutasi@sunserv.kfki.hu

Received 8 September 2010, in final form 10 December 2010
Published 21 February 2011
Online at stacks.iop.org/JPhysD/44/105202

Abstract

The destruction of NO molecules by an Ar plasma jet in a low-pressure (0.2 Torr) reactor is investigated by means of a 3D hydrodynamic model. The density distribution of species created through molecular kinetics triggered by the collision of Ar^+ with NO is calculated, showing that in the case of the most abundant species a quasi-homogeneous density distribution builds up in a large part of the reactor. The conversion of NO into stable O_2 and N_2 molecules is followed under different plasma jet conditions and NO gas flows, and the effect of N_2 addition on NO destruction is studied. It is shown that in the present system the reproduction of NO molecules on the surface through surface-assisted recombination of N and O atoms becomes impossible due to the fast disappearance of N atoms in the jet's inlet vicinity.

1. Introduction

Due to environmental importance, great attention is given to the destruction of NO_x molecules. Toxic nitrogen oxides are present in the emission of combustion gases and are sources of photochemical smog formation, acid rain and the greenhouse effect. The decomposition of NO has been studied by various types of plasmas in different mixtures mostly at atmospheric pressures [1–16]. Many investigations have been carried out in N_2–NO gas mixture discharges in order to study the effect of N_2 on the depletion efficiency, as well as the role of different processes. It has been shown that in N_2–NO discharges a small quantity of NO can be converted into N_2 and O_2 with a high decomposition efficiency [3, 4, 6]. NO molecules are also produced in low-pressure processing systems; they can be the end product—through surface-assisted recombination—of N and O atoms created in low-pressure N_2–O_2 discharges. Therefore the study of NO destruction under low-pressure conditions can also be important.

For NO destruction at low pressures van Helden *et al* [17] have conducted experimental investigations at $p < 100$ Pa using an expanding thermal plasma (ETP) system. The ETP consists of a high-pressure thermal plasma, here namely a dc cascaded Ar arc discharge, and a low-pressure process chamber, where the molecular gases to be dissociated are injected [18, 19]. The large pressure difference between the cascaded arc source (40 kPa) and the process chamber (typically 20–100 Pa) causes a supersonic expansion of the plasma from the nozzle of the cascaded arc into the chamber. The high-velocity ($\approx$2000 m s^{-1}) Ar ions so introduced into the vessel can dissociate the NO molecules [17, 20]. The reduction of the NO molecules in the system under different discharge conditions (arc current) and gas flow rates is determined through mass spectrometry measurements. The NO reduction is shown to increase with the arc current and with a decrease in the NO flow.

In addition to the destruction of NO molecules the ETP system can also be interesting for providing a plasma composed of N_2, O_2 and NO molecules (ground state and excited) and N and O atoms, that can be used for different applications, e.g. plasma sterilization [21, 22], etching [23–25] and oxidation [26]. Since ETP is a system that is not driven by electron-induced ionization and excitation, the plasma composition in the reactor can be varied through parameters that can be more easily controlled than the electron density and energy distribution, such as the molecular gas flow [27].

The aim of this work is to study theoretically the destruction of NO molecules in a low-pressure reactor under different conditions, and to determine the distribution of species densities in the reactor—that are difficult to access

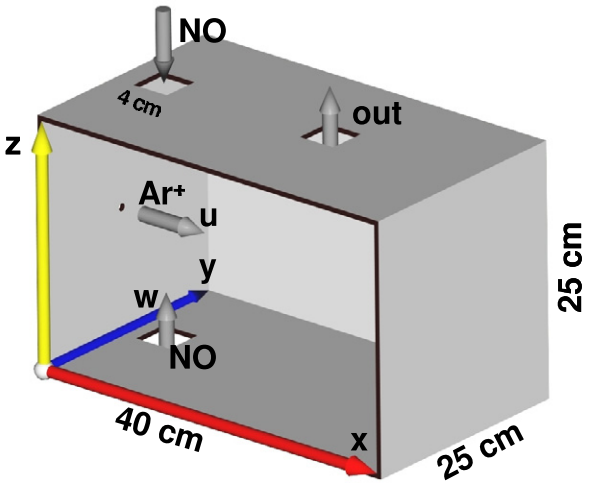

Figure 1. Structure of the 40 cm × 25 cm × 25 cm parallelepipedic reactor. The reactor has three inlets as follows: (i) a 4 × 4 mm^2 square inlet on the left side plate, (ii) a 4 × 4 cm^2 inlet on the top plate and (iii) a 4 × 4 cm^2 inlet on the bottom plate. The 4 × 4 cm^2 gas outlet is positioned on the top plate.

(This figure is in colour only in the electronic version)

experimentally—by means of a 3D hydrodynamic model presented in section 3. As shown by Kaminska *et al* [28]—and as will be discussed in detail in section 4—the velocity and the ionization degree of a plasma jet generated by a dc arc depend on the discharge current. Therefore, to simulate the different discharge conditions, i.e. different arc currents, calculations are performed at different inlet Ar–Ar$^+$ jet mixtures and flows.

2. System set-up

The system investigated in this work has a similar structure to that of van de Sanden *et al* [18] and van Helden *et al* [17]. Here the plasma reactor is a parallelepipedic stainless steel chamber with dimensions of 40 cm × 25 cm × 25 cm (x, y, z). The 4 × 4 mm^2 square inlet, where the high-velocity Ar plasma jet from the dc cascaded arc source enters the reactor, is located in the middle on the left plate, with the 4 × 4 cm^2 gas outlet on the top plate, as shown in figure 1. Two more inlets of 4 × 4 cm^2, which serve as inlets for the molecular gases, are located on the bottom and top plates, respectively, at about 2 cm from the left plate.

3. Hydrodynamic model

The plasma generated at 0.2 Torr in a reactor by a high-velocity Ar plasma jet produced in the external cascaded arc source (not modelled here) is described with a hydrodynamic model, that has been found feasible for the study of the expansion of a supersonic cascaded arc plasma into a low-pressure atmosphere [29]. The three-dimensional hydrodynamic model developed by us is composed of (i) the total mass conservation, (ii) the continuity equations for the different species, (iii) the total momentum conservation equation and (iv) the total energy conservation. The gas is assumed to be a Newtonian fluid. The continuity equations can be written in the following form when the Soret and pressure diffusions are neglected, as well as the Dufour effect [30]:

$$\int_S \rho \boldsymbol{v} \cdot \boldsymbol{n}\,\mathrm{d}S = 0, \tag{1}$$

$$\int_S \rho y_k \boldsymbol{v} \cdot \boldsymbol{n}\,\mathrm{d}S - \int_S \nabla(D_k \rho y_k) \cdot \boldsymbol{n}\,\mathrm{d}S = \int_V m_k S_k^{\mathrm{V}}\,\mathrm{d}V + \int_S m_k S_k^{\mathrm{S}}\,\mathrm{d}S, \tag{2}$$

$$\int_S \rho u_i \boldsymbol{v} \cdot \boldsymbol{n}\,\mathrm{d}S = \int_S \mu\ \mathrm{grad}\ u_i \cdot \boldsymbol{n}\,\mathrm{d}S - \int_S p\boldsymbol{i}_i \cdot \boldsymbol{n}\,\mathrm{d}S, \tag{3}$$

$$\int_S \rho T \boldsymbol{v} \cdot \boldsymbol{n}\,\mathrm{d}S = \int_S \frac{\lambda}{C_p}\ \mathrm{grad}\ T \cdot \boldsymbol{n}\,\mathrm{d}S. \tag{4}$$

Here ρ denotes the total gas density (mass density), $\boldsymbol{v}$ the gas velocity and $\boldsymbol{n}$ the unit vector orthogonal to the S surface and directed outwards. Further, y_k denotes the relative mass density ($y_k = \rho_k/\rho$), D_k and m_k are the diffusion coefficient and the mass of the species k, and S_k^{V} and S_k^{S} represent the source terms associated with volume and surface reactions, respectively. Since S_k^{S} represents a term taking into account surface losses, this term is considered in (2) only on the last grid point at the proximity of the surface. u_i is the velocity in the i direction, p the static pressure, μ the dynamic viscosity, T is the gas temperature, C_p the specific heat at constant pressure and λ the thermal conductivity.

One of the main aims of the model calculations is the determination of the species density distributions in the reactor. The density of species in the system is determined by the chemical kinetics, which is incorporated into the model in the continuity equation of different species through the sources and losses of species resulting from the different chemical reactions, denoted by S_k^{V} in equation (2). The neutral species kinetics in the reactor starts up with the creation of N and O atoms from the dissociation of NO molecules through the following reactions: $Ar^+ + NO \rightarrow Ar + NO^+$ (2.7×10^{-16} m^3 s^{-1} [31]) and $NO^+ + e \rightarrow N + O$ (2×10^{-13} m^3 s^{-1} for the recombination of NO^+ ($v = 0$) with 0.1 eV electrons [32]). In order to simplify our model we do not follow the electrons, which in fact are low-energy electrons with $T_e = 0.1$–0.3 eV, as reported in [17, 18]; thus these electrons do not play an important role in the excitation and ionization kinetics, they are involved only in the recombination processes. The electron dissociative recombination of molecular ion, created in the charge transfer reaction presented above, is very fast [32], therefore we assume that the collision of the Ar^+ ion with NO results in the dissociation of the molecule (i.e. the molecular dissociation occurs in one step $Ar^+ + NO \rightarrow [Ar + NO^+, NO^+ + e] \rightarrow N + O$), producing ground-state N(^{4}S) and O(^{3}P) atoms.

With the O(^{3}P) and N(^{4}S) atoms in the reactor appear the surface processes, which are the atomic recombination. The recombination of atomic species on surfaces, characterized by the surface recombination coefficient, depends on many parameters that can change from one experimental condition to another, e.g. surface material purity, cleanliness, morphology, oxide or nitride type, surface temperature, surface coverage and plasma environment. Therefore it is very difficult to

Table 1. The main reactions taken into account in the hydrodynamic model. The rate coefficients are taken from [22, 36–38]. The rate coefficients for the two- and three-body reactions are in $m^3\,s^{-1}$ and $m^6\,s^{-1}$, respectively, and the decay frequencies are in s^{-1}; T is the temperature in K.

Processes		Rate coefficients
(R1)	$Ar^+ + NO(X) \rightarrow Ar + NO^+$	$2.7 \times 10^{-16}\,m^3\,s^{-1}$
(R2)	$NO^+ + e \rightarrow N(^4S) + O(^3P)$	$2 \times 10^{-13}\,m^3\,s^{-1}$
(R3)	$N(^4S) + wall \rightarrow \frac{1}{2}N_2(X) + wall$	γ
(R4)	$O(^3P) + wall \rightarrow \frac{1}{2}O_2(X) + wall$	γ
(R5)	$N(^4S) + O(^3P) + wall \rightarrow NO(X) + wall$	γ
(R6)	$N(^4S) + NO(X) \rightarrow O(^3P) + N_2(X, v = 3)$	$1.05 \times 10^{-18}T^{0.5}$
(R7)	$N(^4S) + N(^4S) + Ar \rightarrow N_2(B) + Ar$	$0.3 \times 8.27 \times 10^{-46}\exp(T/300)$
(R8)	$N(^4S) + N(^4S) + N_2 \rightarrow N_2(B) + N_2$	$8.27 \times 10^{-46}\exp(T/300)$
(R9)	$N_2(B) + NO \rightarrow N_2(A) + NO$	2.4×10^{-16}
(R10)	$N_2(B) + N_2(X) \rightarrow N_2(A) + N_2(X)$	$0.95 \times 3 \times 10^{-17}$
(R11)	$N_2(B) \rightarrow N_2(A) + h\nu$	2×10^5
(R12)	$N_2(B) + O_2 \rightarrow N_2(X) + O(^3P) + O(^3P)$	3×10^{-16}
(R13)	$N_2(A) + NO(X) \rightarrow N_2(X) + NO(A)$	6.6×10^{-17}
(R14)	$N(^4S) + O_2(X) \rightarrow NO(X) + O(^3P)$	$1.1 \times 10^{-20}T\exp(-3150/T)$
(R15)	$O(^3P) + O(^3P) + Ar \rightarrow O_2(X) + Ar$	$5.21 \times 10^{-47}\exp(900/T)$
(R16)	$O(^3P) + O(^3P) + O_2 \rightarrow O_2(X, a, b) + O_2$	$3.8 \times 10^{-42}\exp(-170/T)/T$
(R17)	$O(^3P) + O(^3P) + O(^3P) \rightarrow O_2 + O(^3P)$	$3.6 \times 10^{-44}T^{-0.63}$
(R18)	$O(^3P) + O_2(X) + O_2 \rightarrow O_3 + O_2$	$6.4 \times 10^{-47}\exp(663/T)$
(R19)	$O(^3P) + O(^3P) + O_2 \rightarrow O_3 + O(^3P)$	$2.1 \times 10^{-46}\exp(345/T)$
(R20)	$O_2(a) + O(^3P) \rightarrow O_2(X) + O(^3P)$	7×10^{-22}
(R21)	$O_3 + O(^3P) \rightarrow O_2(a, b, X) + O_2(X)$	$1.8 \times 10^{-17}\exp(-2300/T)$
(R22)	$O_2(b) + O(^3P) \rightarrow O_2(X) + O(^3P)$	4×10^{-20}
(R23)	$O_2(b) + Ar \rightarrow O_2(X) + Ar$	1.5×10^{-23}
(R24)	$O(^3P) + O_2 + Ar \rightarrow O_3 + Ar$	$3.9 \times 10^{-46}(300/T)^{1.9}$
(R25)	$O_2(a) + Ar \rightarrow O_2(X) + Ar$	1.5×10^{-26}
(R26)	$N(^4S) + O(^3P) + Ar(N_2, O_2) \rightarrow NO(X) + Ar(N_2, O_2)$	$1.76 \times 10^{-43}T^{-0.5}$
(R27)	$N(^4S) + O(^3P) + Ar(N_2, O_2) \rightarrow NO(B) + Ar(N_2, O_2)$	$3.09 \times 10^{-46}(T/300)^{-1.4}$
(R28)	$N(^4S) + O(^3P) + Ar(N_2, O_2) \rightarrow NO(A) + Ar(N_2, O_2)$	$2.12 \times 10^{-46}(T/300)^{-1.24}$
(R29)	$N(^4S) + O(^3P) \rightarrow NO(A)$	$1.18 \times 10^{-23}(T/300)^{-0.35}$
(R30)	$NO(A) \rightarrow NO(X) + h\nu$	4.5×10^6
(R31)	$NO(B) \rightarrow NO(X) + h\nu$	3×10^5
(R32)	$O(^3P) + O_2(X) + N_2 \rightarrow O_3 + N_2$	$5.7 \times 10^{-46}(300/T)^{2.8}$
(R33)	$O(^3P) + NO(X) + N_2(Ar) \rightarrow NO_2(X) + N_2(Ar)$	1×10^{-43}
(R34)	$O(^3P) + NO(X) + O_2 \rightarrow NO_2(X) + O_2$	8.6×10^{-44}
(R35)	$NO(X) + O(^3P) + N_2 \rightarrow NO_2(A) + N_2 \rightarrow NO_2(X) + N_2$	3.7×10^{-44}
(R36)	$NO(X) + O(^3P) + O_2 \rightarrow NO_2(A) + O_2 \rightarrow NO_2(X) + O_2$	3.7×10^{-44}
(R37)	$N(^4S) + NO_2(X) \rightarrow NO(X) + NO(X)$	2.3×10^{-18}
(R38)	$NO_2(X) + O(^3P) \rightarrow NO(X) + O_2(X)$	9.7×10^{-18}

define a proper surface recombination coefficient for atoms (γ) when it comes to modelling of a given experimental condition. The choice of γ has been discussed in detail in our previous work, where the effect of the different γ values has also been investigated [27]. Here we just recall, that for the stainless steel surface in the case of N atoms we choose $\gamma_N = 7.5 \times 10^{-2}$ [27, 33, 34], while in the case of O atoms we choose $\gamma_O = 7 \times 10^{-2}$ [35]. The losses of atoms are calculated according to the equation

$$S_k^S = -\gamma_k \frac{v_k}{4} n_k, \tag{5}$$

where $v_k = \sqrt{8k_B T/\pi m_k}$ is the average velocity of k atoms and γ_k is the corresponding atomic surface loss probability. The N and O atoms on the surface can recombine either into N_2 and O_2, respectively, or into NO molecules (table 1 (R3)–(R5)). The experimentally determined γ surface recombination coefficient includes all the possible surface reactions, thus making it possible to describe the loss and creation of species on the surface without a detailed surface kinetic model. However, it gives no possibility to decide which recombination process occurs, i.e. whether the N atoms recombine into N_2 or into NO together with the O atoms. The implementation of the atomic surface losses and the choice of the surface elementary processes were discussed in detail in [27].

Table 2. The diffusion coefficients given in $m^2\,s^{-1}$ are taken from [39–42]. The temperature T is in K and the pressure p in Pa.

$D(Ar) = 3.5 \times 10^{-4}\frac{T^{1.5}}{p}$
$D(O_2(a, b)) = 3.87 \times 10^{-3}\frac{T}{p}$
$D(O_2, O_3) = 8.8 \times 10^{-5}\frac{T^{1.75}}{p}$
$D(O) = 5.85 \times 10^{-4}\frac{T^{1.5}}{p}$
$D(N_2(X, A, B)) = 3.99 \times 10^{-4}\frac{T^{1.5}}{p}$
$D(N) = 6 \times 10^{-4}\frac{T^{1.75}}{p}$
$D(NO(X, A, B)) = 1.42 \times 10^{-4}\frac{T^{1.69}}{p}$
$D(N_2(X, A, B)) = 3.99 \times 10^{-4}\frac{T^{1.5}}{p}$
$D(NO_2) = 6.24 \times 10^{-6}\frac{T^{1.75}}{p}$

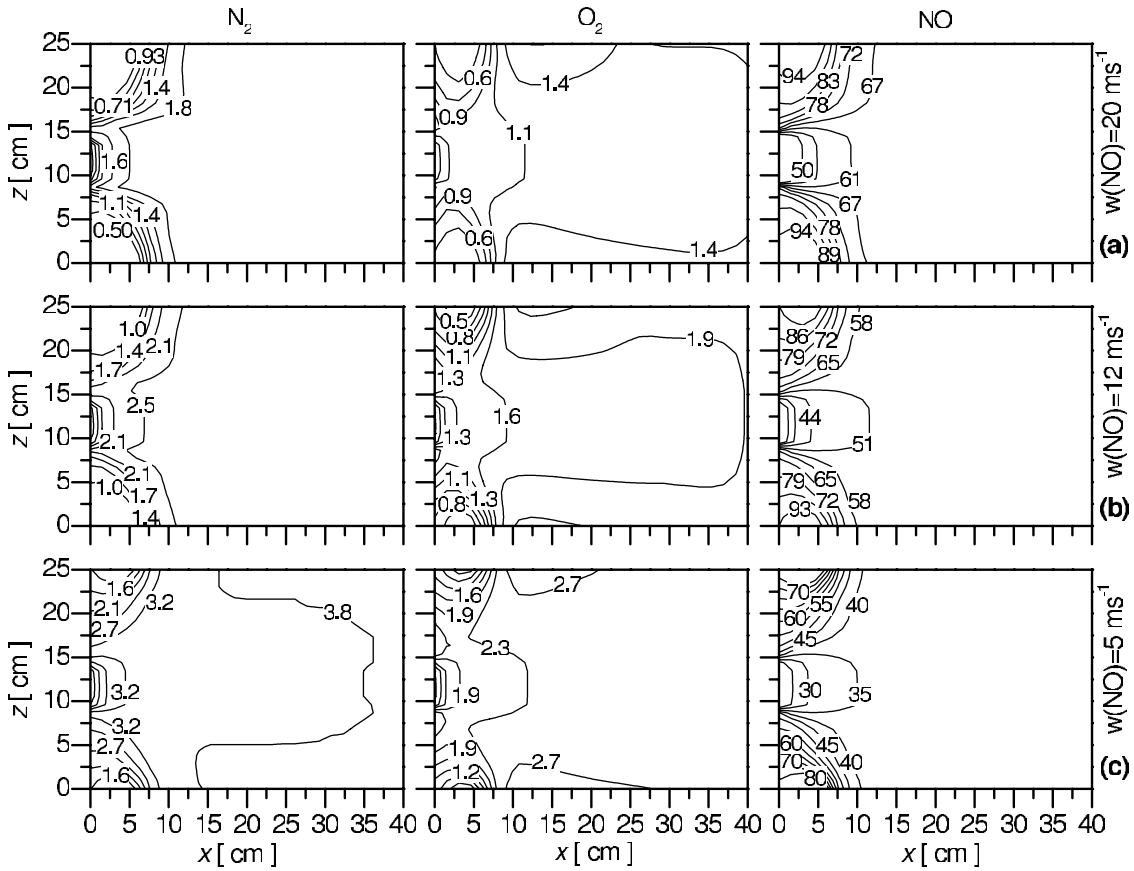

Figure 2. The distribution of species abundances (%) in the x–z vertical plane at $y = 12.5$ cm for the following NO inlet velocities: (*a*) 20 m s^{-1}, (*b*) 12 m s^{-1} and (*c*) 5 m s^{-1} when the Ar jet inlet velocity is 2000 m s^{-1} and the ionization degree is 15%. Columns 1 to 3 are for different molecules.

With the appearance of N_2 and O_2 molecules in addition to the O(^{3}P) and N(^{4}S) atoms further gas phase reactions can take place in the reactor filled with NO, which give rise to excited and newly formed molecules. First of all the N and O atoms can also recombine in the gas phase through two-body, as well as three-body processes. The most important process for the N(^{4}S) atoms in a system with predominant NO molecules is the dissociative collision with NO(X) giving rise to N_2 and O(^{3}P) (R6). The three-body recombination of N(^{4}S) can result in excited $N_2(B)$ molecules (R7) and (R8), which through quenching by NO, N_2 and radiative decay turn into metastable $N_2(A)$ molecules (R9)–(R11). The N(^{4}S) atoms can further contribute to the formation of ground-state NO(X) molecules through two-body collision with $O_2(X)$ (R14). In the case of O(^{3}P) atoms, their three-body recombination can result in ground-state O_2 and excited $O_2(a)$ and $O_2(b)$ molecules, as well as O_3 (R15)–(R19). The O atoms together with the N atoms can also contribute to the formation of NO(X), NO(A) and NO(B) molecules through the two-body and three-body re-association processes in the presence of Ar, N_2 and O_2 (R29), (R26)–(R28). And finally, the NO molecules participate in the creation of $NO_2(X)$ through the three-body re-association with O(^{3}P) in the presence of N_2, O_2 and Ar, respectively (R33)–(R36). A full list of gas phase reactions that govern the molecular kinetics of an Ar–NO–N_2–O_2 system has been given in our previous publication [27].

The distribution of species densities in the reactor in addition to the chemical reactions is influenced by the gas flow and the diffusion of different species. The diffusion coefficients chosen are presented in table 2. The transport data necessary as input data for the model are taken from [38, 43]. The inlet and wall temperatures required for the energy conservation equation are defined as follows: the inlet temperature of the Ar jet is taken to be 12 000 K according to Selezneva *et al* [29], while the inlet NO and wall temperatures are chosen as 300 K [29].

As concerns the solution method, the model is solved using the algorithm given by Ferziger and Perić [44]. The equations are discretized using the finite volume method. The linear algebraic equation system so obtained is then solved with Stone's method iteratively using the multigrid method. In our solution three grid levels are used, the finest grid has $80 \times 40 \times 80$ control volumes.

4. Results and discussion

One of the recent modelling investigations of an argon plasma jet generated by a dc arc is that of Kaminska *et al* presented in [28]. They discuss the dc current dependence of jet's velocity in different parts of the divergent nozzle, as well as the ionization degree of the plasma jet. They have shown that in the 60–140 A current range at the end of the nozzle

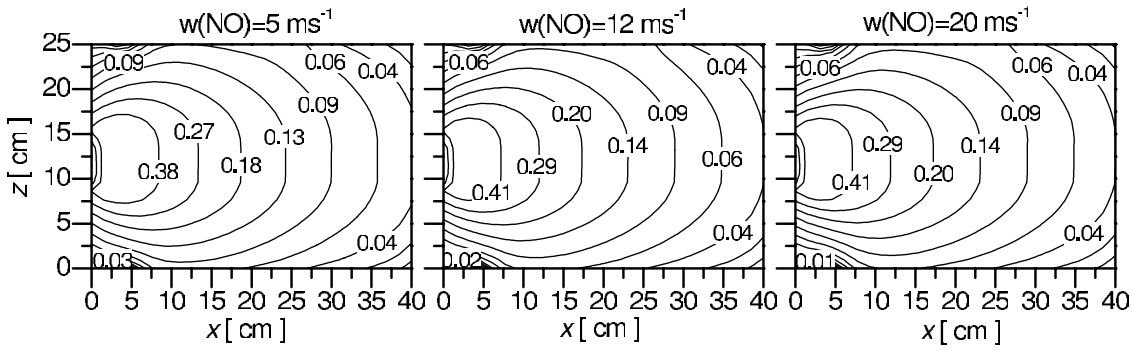

Figure 3. The distribution of O atom abundance (%) in the x–z vertical plane at $y = 12.5$ cm for different NO inlet velocities from column 1 to 3, when the Ar jet inlet velocity is 2000 m s^{-1} and the ionization degree is 15%.

velocities between 3500 and 5500 m s^{-1} are obtained, while the ionization degree can reach 60%. Regarding the ionization degree, the calculations of Beulens *et al* [45] show that it is about 15% at 60 A dc current and increases up to ≈75% at 200 A. Along with these results we have conducted systematic calculations varying the jet velocity between 2000 m s^{-1} (estimated by Engeln *et al* [19]) and 3500 m s^{-1}, and the ionization degree in the 15–35% range, as an attempt to simulate the lower current conditions.

Figure 2 shows the distribution of relevant species—NO, N_2 and O_2 molecules created through the recombination of atoms provided by the dissociation of NO—in the reactor at three different NO inlet velocities when the Ar jet inlet velocity is set to 2000 m s^{-1} and the ionization degree to 15%. The distributions are shown in the vertical symmetry plane of the reactor, i.e. x–z vertical plane at $y = 12.5$ cm. The figures show that in the case of these species at ≈10 cm from the jet entrance quasi-homogeneous density distributions are built up. On the other hand, along the same distance the density of N atoms becomes negligible. The N atoms created from NO dissociation cannot survive long, since they collide with the non-dissociated NO molecules and recombine into N_2 giving rise to O atoms. As a result the reproduction of NO molecules through surface processes, i.e. surface recombination of N and O atoms, becomes impossible. The density of O atoms is about one order of magnitude lower than that of O_2; their recombination into O_2 occurs through a surface recombination process, which results in a decrease in density distribution from the jet's entrance vicinity to the walls, as illustrated in figure 3. With increasing NO inlet velocity a slight increase in O atom abundance can be observed at the entrance vicinity; however, in the big part of the reactor very similar abundances are obtained for different NO inlet flows.

Figure 2 also clearly shows that by decreasing the NO flow—from figure 2(*a*) to (*c*)—the dissociation of NO molecules becomes more effective, i.e. the N_2 and O_2 abundances increase, while that of NO decreases. To have a more clear idea about the depletion of NO molecules under different conditions we present the reduced O_2 and N_2 mass density fraction, $([N_2] + [O_2])/([N_2] + [O_2] + [NO])$ [17], as a function of NO inlet velocities as shown in figure 4. First of all we investigate how the conversion of NO into N_2 and O_2 evolves with the ionization degree of the jet. The full symbols

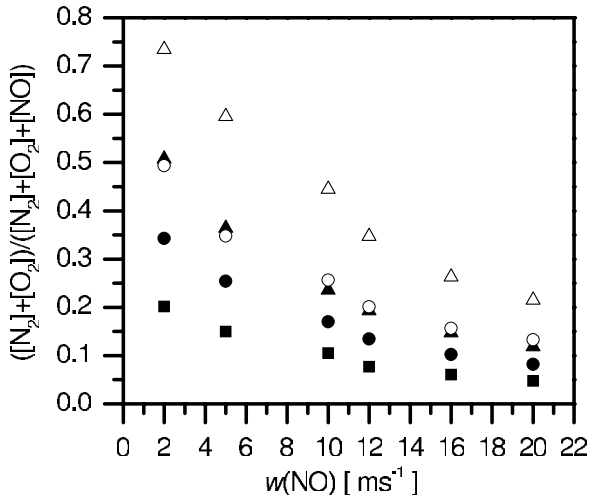

Figure 4. Reduced O_2 and N_2 mass density fraction as a function of NO inlet flow. The full symbols represent the case of 2000 m s^{-1} velocity plasma jet with different ionization degrees 15% (■), 25% (●) and 35% (▲). The open symbols represent two cases of higher jet velocity as follows: 3000 m s^{-1} with 25% ionization degree (○) and 3500 m s^{-1} with 35% Ar^+ (△).

in figure 4 represent the reduced O_2 and N_2 density fraction for three different ionization degrees: 15%, 25% and 35%, when the jet velocity is kept constant at 2000 m s^{-1}. As already suggested by the density distributions we can observe an increase in the NO conversion with decreasing NO flow, shown experimentally also by van Helden *et al* (figure 12 in [17]). Similarly, the NO conversion increases also with the ionization degree of the plasma jet, which is in concordance with the NO conversion observed experimentally with the arc current (one can refer to figure 13 in [17]). According to the calculations of Kaminska *et al* [28], it is not only the ionization degree that increases with the arc current, but also the jet velocity. Accordingly, in the following when choosing the ionization degree as 25% we increase the jet velocity to 3000 m s^{-1}, while in the case of 35% to 3500 m s^{-1}. The results thus obtained are illustrated by the open symbols presented in figure 4. As expected, the increase in the jet velocity, which ensures a higher Ar^+ inlet mass flow, results in a more efficient NO destruction. In this way the highest conversion rate obtained is 75% in comparison with 50% resulting from the previous conditions.

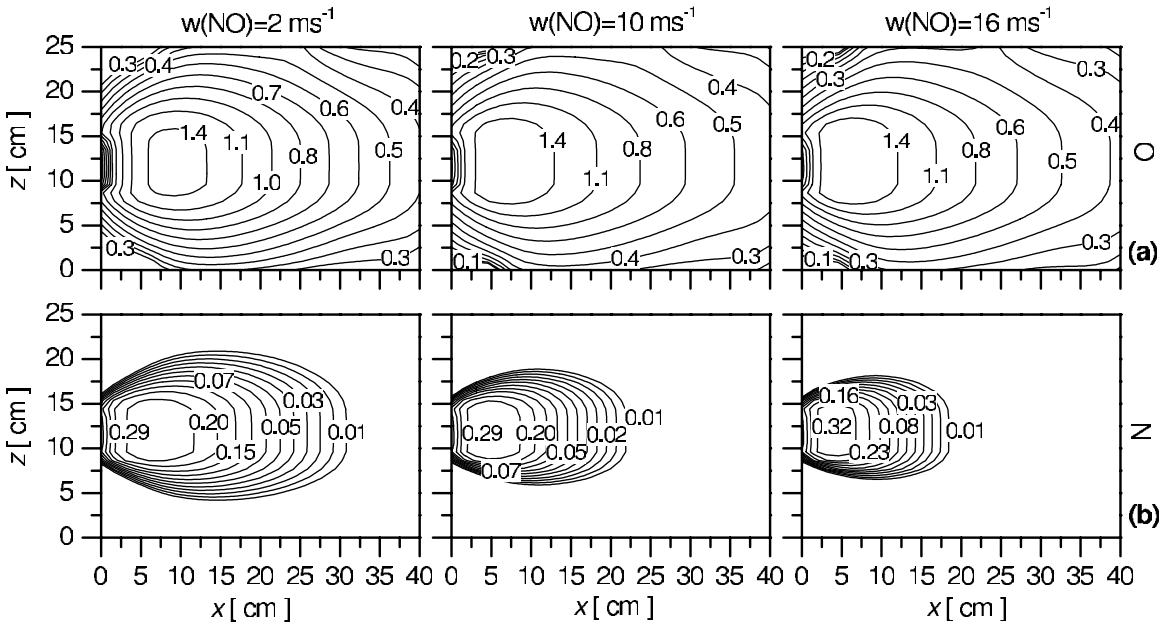

Figure 5. The distribution of (*a*) O atom and (*b*) N atom abundances (%) in the x–z vertical plane at $y = 12.5$ cm for different NO inlet velocities from column 1 to 3, when the Ar jet inlet velocity is 3500 m s^{-1} and the ionization degree is 35%. Abundances lower than 0.01% are omitted in the figure.

By increasing the ionization degree of the cascaded arc, in addition to the more efficient NO destruction, higher atomic densities are also expected. Figure 5 shows the distribution of the N and O atom abundances for different NO inlet velocities in the case of 3500 m s^{-1} jet velocity and 35% ionization degree. Indeed, considerably higher O atom abundances (it decreases from 1.4% to 0.3% to the walls) are obtained than in the case of lower ionization degree jet, for comparison one should refer to figure 3. It is also interesting to examine the density distribution of atoms in the reactor. While the distribution of O atom abundances is very similar for the different NO inlet flows, the N atoms show a different behaviour with the flow. With increasing NO inlet flow the N atoms are quenched much faster due to collision with NO molecules (R6).

Assuming a reactor surface that has a much lower atomic recombination probability, such as $\gamma = 10^{-3}$, we can examine the influence of surface recombination on the atomic density distributions. Figure 6 shows the N and O atom abundances in the reactor for the lower NO flow investigated here. We can notice that the surface recombination has no effect on the N atom density, while in the case of O atoms we can observe considerable increase in the density compared with the surface with higher recombination probability, see figure 5(*a*) first column.

Addition of N_2. The destruction of NO at atmospheric pressure has been widely investigated in N_2–NO gas mixture discharges, achieving a better efficiency with N_2 addition. In the active discharge for this mixture the main NO destruction mechanism is the collision of NO with N atoms [4]. However, in the ETP both charge transfer and electron-induced dissociative recombination ($Ar^+ + NO \rightarrow Ar + NO^+$ and $NO^+ + e \rightarrow N + O$), and the N-atom-induced dissociation ($NO + N \rightarrow N_2 + O$) processes play comparable roles.

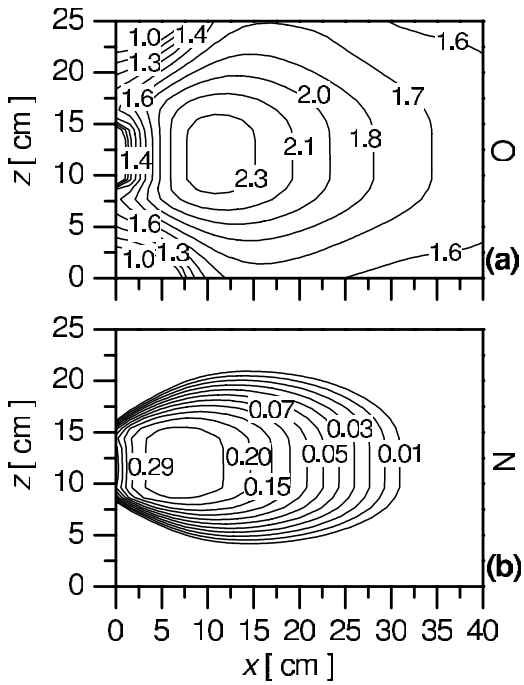

Figure 6. The distribution of (*a*) O atom and (*b*) N atoms abundances (%) in the x–z vertical plane at $y = 12.5$ cm when the NO inlet velocity is 2 m s^{-1}, Ar jet inlet velocity is 3500 m s^{-1}, the ionization degree is 35% and the atomic surface recombination probabilities are chosen as 10^{-3}. Abundances lower than 0.01% are omitted in the figure.

In the present system N_2 has been introduced by replacing the NO gas flow with N_2 gas flow at the bottom plane inlet (see figure 1). With the addition of N_2 to the system, the dissociation reactions of N_2 and NO through charge transfer and electron-induced dissociative recombination become competing reactions. In this case the N atoms can be created

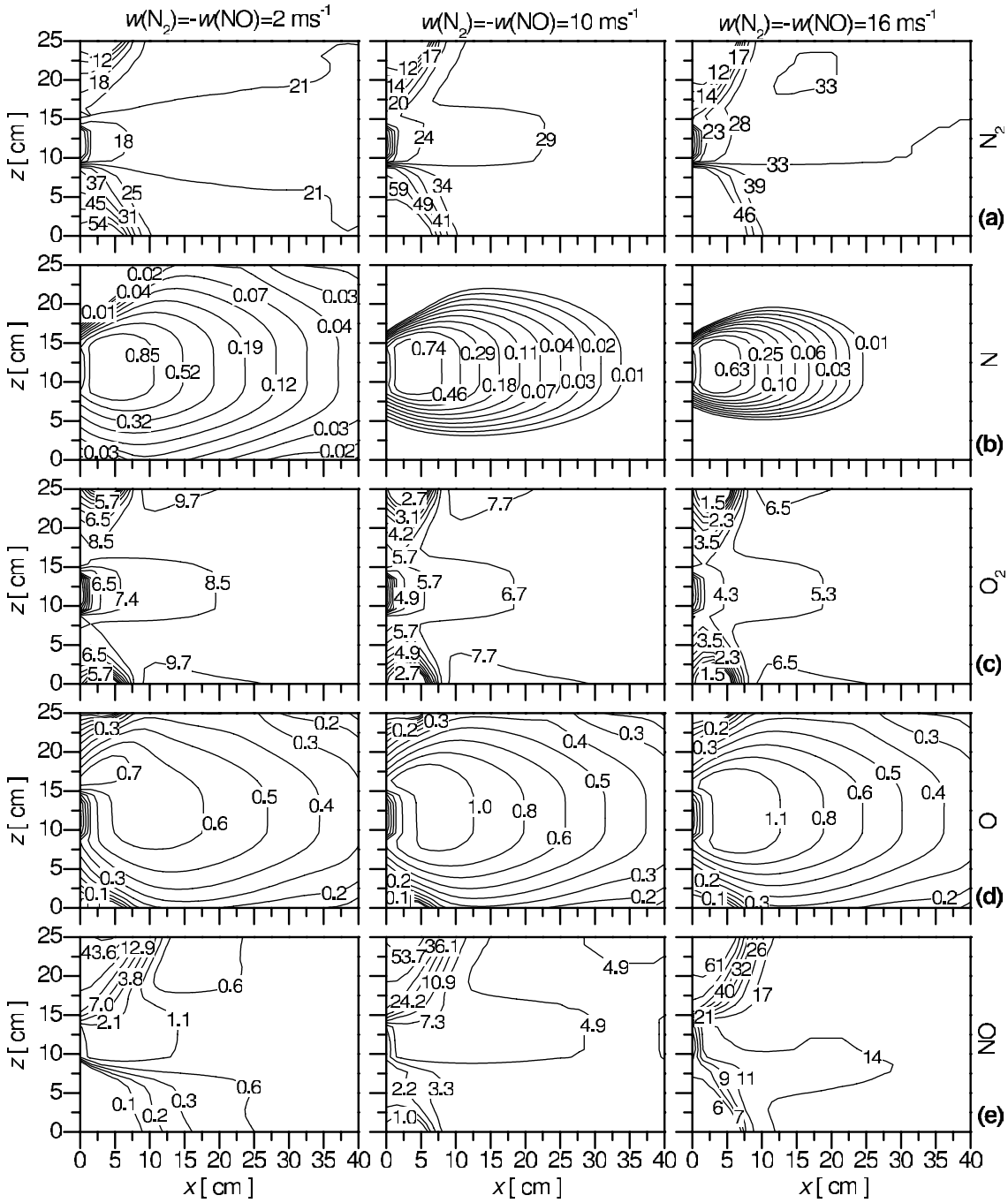

Figure 7. The distribution of (*a*) N_2, (*b*) N, (*c*) O_2, (*d*) O and (*e*) NO abundances (%) in the x–z vertical plane at $y = 12.5$ cm for different $w(N_2) = -w(NO)$ inlet velocities from column 1 to 3, when the Ar jet inlet velocity is 3500 m s^{-1} and the ionization degree is 35%.

through two different reaction paths: (i) $Ar^+ + NO \rightarrow Ar + NO^+$ (2.7×10^{-16} m^3 s^{-1} [31]), $NO^+ + e \rightarrow N + O$ (2×10^{-13} m^3 s^{-1} [32]) and (ii) $Ar^+ + N_2 \rightarrow Ar + N_2^+$ (4.45×10^{-16} m^3 s^{-1} [46]), $N_2^+ + e \rightarrow N + N$ (2×10^{-13} m^3 s^{-1} [47]), respectively. Again for simplicity (see section 3), in order not to follow also the slow electrons, and since the electron recombination dissociation reaction is very fast, the dissociation of molecules is assumed to occur in one step as follows: $Ar^+ + NO \rightarrow [Ar + NO^+, NO^+ + e] \rightarrow N + O$ and $Ar^+ + N_2 \rightarrow [Ar + N_2^+, N_2^+ + e] \rightarrow N + N$.

Figure 7 represents the distribution of species abundances in the reactor's symmetry plane. In the case of N atoms, compared with the pure NO case, considerably higher densities are obtained, although still abundances less than 1% are achieved, figure 7(*b*). In this case nevertheless there is an N atom density built up at the reactor's wall vicinity; however, the contribution of N atoms to the surface formation of molecules is negligible. With increasing molecular gas flows we can observe faster quenching of N atoms similarly to the case of pure NO inlet. For the O_2 molecules the higher abundances obtained at lower molecular flows predict the higher depletion rate of NO molecules, figure 7(*c*). Contrary to the molecules, the O atom density, (figure 7(*d*)) increases with the molecular gas flow; however, for each case it reaches similar values at the wall.

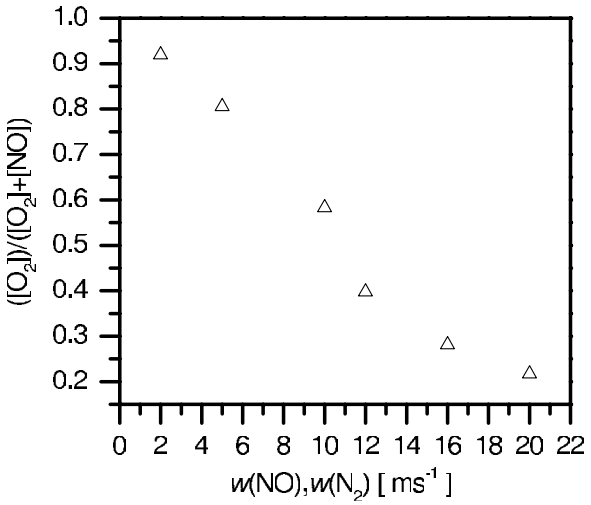

Figure 8. Reduced O_2 mass density fraction as a function of equally set NO and N_2 inlet flows in the case of 3500 m s^{-1} velocity plasma jet with 35% ionization degree.

We follow the conversion of NO in this case through the reduced O_2 density defined as $([O_2])/([O_2] + [NO])$ presented in figure 8 in the case of Ar plasma jet velocity 3500 m s^{-1} and ionization degree 35%. Although, a one to one comparison cannot be made with the reduced densities defined in the case of pure NO (figure 4), obviously with N_2 addition the depletion of NO becomes more efficient. With N_2 addition although the dissociation reactions of N_2 and NO through charge transfer and electron-induced dissociative recombination are competing reactions, the N atoms resulting from N_2 dissociation contribute strongly to the NO depletion through the (R6) process.

5. Concluding remarks

We have studied the destruction of NO molecules by an Ar plasma jet in a low-pressure $p = 0.2$ Torr reactor. The Ar plasma jet produced by a dc cascaded arc (not studied here) is introduced through a 4×4 mm^2 orifice into the low-pressure reactor. NO gas is fed into the reactor through two inlets placed symmetrically on the top and on the bottom planes. Through the molecular kinetics triggered by the collision of Ar^+ with NO several species are created in the reactor. To calculate the density distributions of these species we have used a 3D hydrodynamic model. Depending on the dc current of the arc discharge the ionization degree of the plasma jet, as well as its velocity, can vary in a wide range. With an attempt to simulate the lower arc dc current situations we varied the jet velocity between 2000 and 3500 m s^{-1}, and the ionization degree in the 15–35% range.

Calculations have shown that in the case of the most abundant species, such as N_2, O_2 and NO, a quasi-homogeneous density distribution builds up in a large part of the reactor, while the N atoms disappear within a few centimetres. In the case of O atoms we obtain a decreasing density profile from the vicinity of jet entrance to the walls. We have shown that due to the fast disappearance of N atoms through their collision with NO molecules, the reproduction of NO molecules on the wall through the surface recombination of N and O atoms becomes impossible.

We have followed the conversion of NO into stable O_2 and N_2 molecules under different plasma jet conditions and NO gas flows, and have shown that the NO reduction becomes more efficient with decreasing NO inlet flow and increasing plasma jet ionization degree and velocity, which is equivalent to an increase in the dc arc current. By adding N_2 to NO—replacing one of the NO inlet flows with N_2—we have observed a more efficient NO destruction. Although in this way more nitrogen has been added to the system, the N atom abundances do not exceed 1%.

Acknowledgments

The work has been supported by the Hungarian Science Foundation OTKA through project F-67556 and by the Janos Bolyai Research Scholarship of the Hungarian Academy of Sciences.

References

[1] Clements J C, Mizuno A, Finney W C and Davis R H 1989 *IEEE Trans. Indust. Appl.* **25** 62
[2] Masuda S and Nakao H 1990 *IEEE Trans. Indust. Appl.* **26** 374
[3] Penetrante B M, Hsiao M C, Merritt B T, Vogtlin G E and Wallman P H 1995 *Appl. Phys. Lett.* **67** 3096
[4] Penetrante B M, Hsiao M C, Merritt B T, Voglin G E and Wallman P H 1996 *Appl. Phys. Lett.* **68** 3719
[5] Kiyokawa K, Matsuoka H, Itou A, Hasegawa K and Sugiyama K 1999 *Surf. Coat. Technol.* **112** 25
[6] Gal A, Kurahashi M and Kuzumoto M 1999 *J. Phys. D: Appl. Phys.* **32** 1163
[7] Wojtowicz M A, Miknis F P, Grimes R W, Smith W W and Serio M A 2000 *J. Hazard. Mater.* **74** 81
[8] Baeva M, Gier H, Pott A, Uhlenbusch J, Höschele J and Steinwandel J 2001 *Plasma Chem. Plasma Process.* **21** 225
[9] Tsuji M, Nakano K, Kumagae J, Matzuzaki T and Tsuji T 2003 *Surf. Coat. Technol.* **165** 296
[10] Chang M B, Kushner M J and Rood M J 1992 *Env. Sci. Technol.* **26** 777
[11] Gentile A C and Kushner M J 1995 *J. Appl. Phys.* **78** 2074
[12] Dorai R and Kushner M J 2003 *J. Phys. D: Appl. Phys.* **36** 1075
[13] Nusca M J, Rosocha L A and Herron J T 2000 *38th Aerospace Sciences Meeting and Exhibit (Reno, NV, 10–13 January 2000)* AIAA 2000-0719
[14] Eichwald O, Guntoro N A, Yousfi M and Benhenni M 2002 *J. Phys. D: Appl. Phys.* **35** 439
[15] Orlandini I and Riedel U 2000 *J. Phys. D: Appl. Phys.* **33** 2467
[16] Filimonova E A, Kim Y, Hong S H and Song Y H 2002 *J. Phys. D: Appl. Phys.* **35** 2795
[17] van Helden J H, Zijlmans R A B, Schram D C and Engeln R 2009 *Plasma Sources Sci. Technol.* **18** 025020
[18] van de Sanden M C M, Severens R J, Kessels W M M, Meulenbroeks R F G and Schram D C 1998 *J. Appl. Phys.* **84** 2426
[19] Engeln R, Mazouffre S, Vankan P, Schram D C and Sadeghi N 2001 *Plasma Sources Sci. Technol.* **10** 595
[20] Zijlmans R A B, Welzel S, Gabriel O, Yagci G, van Helden J H, Röpcke J, Schram D C and Engeln R 2010 *J. Phys. D: Appl. Phys.* **43** 115204
[21] Ricard A and Monna V 2002 *Plasma Sources Sci. Technol.* **11** A150
[22] Kutasi K, Saoudi B, Pintassilgo C D , Loureiro J and Moisan M 2008 *Plasma Process. Polym.* **5** 840

[23] Lin T H, Belser M and Tzeng Y 1988 *IEEE Trans. Plasma Sci.* **16** 631
[24] Brussaard G J H, Letourneur K G Y, Schaepkens M, van de Sanden M C M and Schram D C 2003 *J. Vac. Sci. Technol.* B **21** 61
[25] Hody V, Belmonte T, Pintassilgo C D, Poncin-Epaillard T, Czerwiec T, Henrion G, Segui Y and Loureiro J 2006 *Plasma Chem. Plasma Process.* **26** 251
[26] Yasuda Y, Zaima S, Kaida T and Koide Y 1990 *J. Appl. Phys.* **67** 2603
[27] Kutasi K 2010 *J. Phys. D: Appl. Phys.* **43** 055201
[28] Kaminska A, Lopez B, Izrar B and Dudeck M 2008 *Plasma Sources Sci. Technol.* **17** 035018
[29] Selezneva S E, Boulos M I, van de Sanden M C M, Engeln R and Schram D C 2002 *J. Phys. D: Appl. Phys.* **35** 1362
[30] Kutasi K, Pintassilgo C D and Loureiro J 2009 *2nd Int. Workshop on Non-equilibrium Processes in Plasmas and Environmental Science (Belgrade, Serbia) J. Phys.: Conf. Ser.* **162** 012008
[31] Shul R J, Upschulte B L, Passarella R, Keesee R G and Castleman A W Jr 1987 *J. Phys. Chem.* **91** 2556
[32] Florescu-Mitchell A I and Mitchell J B A 2006 *Phys. Rep.* **430** 277
[33] Marković V Lj, Petrović Z Lj and Pejović M M 1995 *Japan. J. Appl. Phys.* **34** 2466
[34] Adams S F and Miller T A 2000 *Plasma Sources Sci. Technol.* **9** 248
[35] Mozetič M and Zalar A 2000 *Appl. Surf. Sci.* **158** 263
[36] Guerra V and Loureiro J 1999 *Plasma Sources Sci. Technol.* **8** 110
[37] Pintassilgo C D, Loureiro J and Guerra V 2005 *J. Phys. D: Appl. Phys.* **38** 417
[38] Belmonte T, Czerwiec T, Gavillet J and Michel H 1997 *Surf. Coat. Technol.* **97** 642
[39] Tachibana K and Phelps A V 1981 *J. Phys. Chem.* **75** 3315
[40] Lide D R 1994 *Handbook of Chemistry and Physics* 75th edn (Boca Raton, FL: CRC Press)
[41] Morgan J E and Schiff H I 1964 *Can. J. Chem.* **42** 2300
[42] Bockel S, Belmonte T, Michel H and Ablitzer D 1997 *Surf. Coat. Technol.* **97** 618
[43] Kutasi K, Pintassilgo C D, Coelho P J and Loureiro J 2006 *J. Phys. D: Appl. Phys.* **39** 3978
[44] Ferziger J H and Peric M 2002 *Comput. Methods Fluid Dynamics* 3rd rev. edn (Berlin: Springer)
[45] Beulens J J, Milojevic D, Schram D and Vallinga P M 1991 *Phys. Fluids* B **3** 2548
[46] Viaggiano A A and Morris R A 1993 *J. Chem. Phys.* **99** 3526
[47] Peterson J R *et al* 1998 *J. Chem. Phys.* **108** 1978